JOURNAL OF MECHANICAL ENGINEERING AND SCIENCES (JMES)
ISSN: 2289-4659 e-ISSN: 2231-8380
VOL. 14, ISSUE 3, 6971 – 6981
DOI: https://doi.org/10.15282/jmes.14.3.2020.01.0546

ORIGINAL ARTICLE

Experimental comparison of sinusoidal motion and non-sinusoidal motion of rise-dwell-fall-dwell in a Stirling engine

H.M. Wong[1] and S.Y. Goh[1]

[1] Department of Mechanical and Materials Engineering, Lee Kong Chian Faculty of Engineering and Science, Universiti Tunku Abdul Rahman, Jalan Sungai Long, Bandar Sungai Long, Cheras 43300, Kajang, Selangor, Malaysia
Phone: +60390860288; Fax: +60390198868

ABSTRACT – The Stirling engine is deemed to play a role in the near future of power generation. However, there is a large performance difference between the real and ideal Stirling engine. The use of sinusoidal motion for both displacer and piston in current applications is one of the reasons for this difference as it limits heat transfer. This paper investigated the use of non-sinusoidal rise-dwell-fall-dwell (RDFD) motion on both displacer and piston to improve the performance of a real Stirling engine and compared it to the conventional sinusoidal motion crankshaft driven Stirling engine. A gamma configuration Stirling engine test rig with a data acquisition system was constructed for this investigation. Among the four flywheels with each specifically designed cam profile tested, one was with sinusoidal motion while the remaining three were non-sinusoidal for comparison. The use of non-sinusoidal RDFD cam with 135° displacer dwell improved more than 36% thermal efficiency over sinusoidal motion crankshaft Stirling engine.

ARTICLE HISTORY
Revised: 13th Apr 2020
Accepted: 14th Apr 2020

KEYWORDS
Stirling engine;
non-sinusoidal motion;
rise-dwell-fall-dwell motion;
thermal efficiency;

INTRODUCTION

The Stirling engine had been considered to be one of the many candidates as a clean power generator for the future. It is a regenerative closed cycle hot air engine, able to run off from any sources of heat energy. Benefits of using Stirling engines are multi-fueled capability, low fuel consumption, high efficiency, clean combustion, low noise level and low temperature operation [1]. Figure 1(a) showed an ideal Stirling cycle [2] in a gamma configured Stirling engine and Figure 1(b) showed its four ideal gas processes (two constant volume regenerative heat transfer and two isothermal). A displacer shuttles the working gas trapped in the engine, between the hot and cold end where heat is continuously added and removed at its respective ends. Exposure of working gas to the hot and cold end would expand (process 3-4) and compress it (process 1-2). A piston extracts mechanical work from the expansion and compression of the working gas. A regenerator is located between the hot and cold end, temporarily stores and discards heat as hot and cold working gas passes through (process 4-1 and 2-3), reducing the amount of needed heat input while improving thermal efficiency of the Stirling engine.

The real Stirling engine however didn't operate as represented in the ideal thermodynamic cycle. Stirling cycle is an ideal cycle where it operates with four ideal reversible gas processes and uses an inviscid working fluid in an engine with ideal engine geometry (all engine volumes participate in heat exchange and gas expansion). The real Stirling engine however operates with irreversible polytropic gas processes and uses a viscous working fluid in an engine with real engine geometry (has volumes in the heat exchangers and channels connecting all of its components) [3, 4].

Recent researches in Stirling engine was found encompassing both simulation work and experimental work. Simulation work enables detailed study of Stirling engine design parameters [5]. It is used for the task of optimization [6 – 13], exploration of new design or concept [14 – 19] as well as parametric study of Stirling engines [5, 20, 21]. Experimental study focuses on validation and performance testing of existing or new Stirling engine design [9, 16].

There was lesser amount of research in the area of Stirling engine displacer and piston motion control. Since the first Stirling engine in 1816, the drive mechanism of choice is a crank-slider and lever arrangement. There was some variation to this but they all generates displacer and piston motions that is near sinusoidal motion [2, 4, 22]. Comparatively, in an ideal Stirling cycle, there is a discontinuation of motion of both displacer and piston to perform the four ideal gas processes, as shown in Figure 1 (a) and (b) [4]. Therefore, all Stirling engines with near sinusoidal displacer and piston motion are a compromise between theoretical need and mechanical capability in terms of its drive mechanism. It is also due to this inability to stop momentarily of the displacer and piston, performance of the practical Stirling engines is lowered. Ranieri et. al (2018) [23] found that the usage of sinusoidal motion in an alpha type Stirling engine provides only 65.9% of the efficiency for ideal cyclic motion. The same effect was seen for beta and gamma type Stirling engine. Červenka (2016) [3] found that power dropped from 8.51 kW in an ideal cycle to 1.54 kW in a sinusoidal real cycle, through simulation.

*CORRESPONDING AUTHOR | H.M. Wong | ✉ wonghm@utar.edu.my

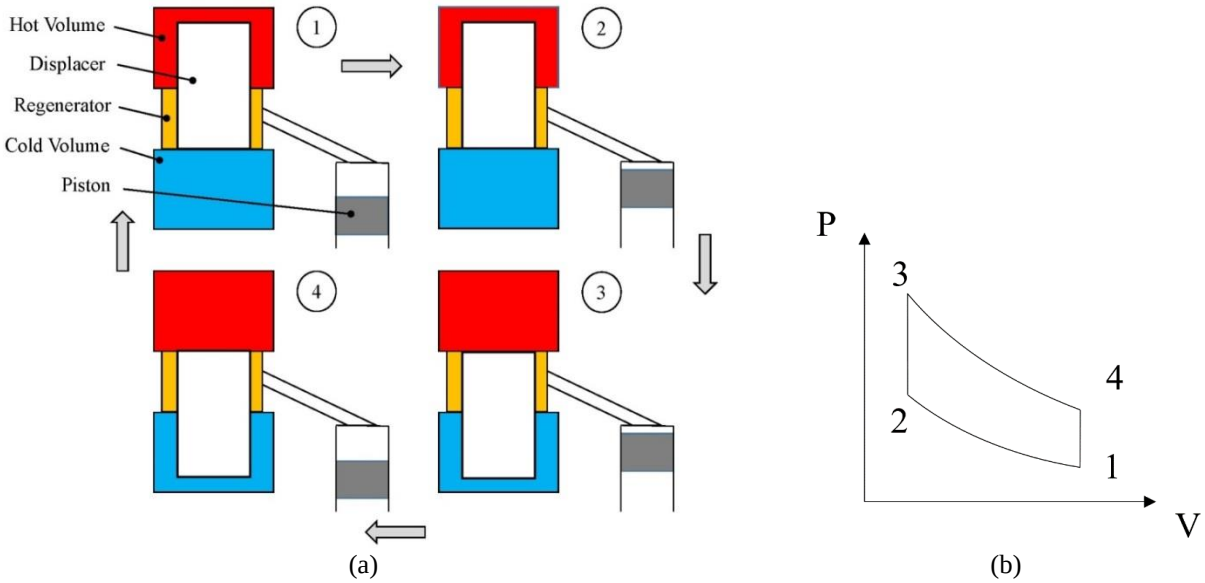

Figure 1. Ideal Stirling cycle as represented in; (a) schematic diagram of gamma configured Stirling engine, (b) PV diagram

There were research efforts to bridge the gap between the ideal Stirling cycle and real Stirling engine cycle in terms of the motion of its displacer and piston. The key was to accept non-perfect heat exchanging and regenerating. The effort is to maximize the ability to exchange heat and regeneration. Heat exchanging capability can be improved by utilizing appropriate materials [24], size or dimensions [25, 26] and type or fin shape [26, 27]. Non-sinusoidal motion of displacer could isolate the effect of heating and cooling the working fluid at the same time by shuttling most of the working fluid to either end of the heat exchangers and having it remain there for a longer period of time. This in return can exchange more heat into the working fluid as it has more mass on that end and little working fluid mass on the other end. Briggs (2015) [28] manipulated the sinusoidal volume change of a free-piston Stirling engine electrically and effectively made the engine runs with a non-sinusoidal volume change. Thermodynamic power was found increased by 14%. Gopal (2012) [29] decoupled the displacer in a modified Stirling engine and drives the displacer with a programmable linear motor. The displacer was given a non-sinusoidal motion while the power piston followed a sinusoidal motion. With a 50% displacer dwell, efficiency was increased by 15% compared with sinusoidal displacer motion. Craun and Bemiah (2015) [19] found more than 40% improvement in performance with the usage of displacer non-sinusoidal motion compared to sinusoidal motion, through simulation. Fang et al. (1996) [30] theorizes the used of epileptic gears to achieve better approximate ideal volume change. Podešva and Poruba (2016) [31] investigated three types of link mechanism that can dwell at the top most and bottom most position that could possibly increase its effectiveness. Jaśkiewicz et al. (2013) [32] suggested to utilize a cam mechanism that could prolong the period of heating and cooling while the transitory is shorter to improve performance. Van de Ven (2009) [33] suggested some special control involving hydraulic valves for a liquid piston Stirling engine that could matches an ideal Stirling cycle. Cullen and McGovern (2011) [15] suggested the possibility of using electronically controlled motor / generator, rack and pinion gearing to oscillate pistons in an alpha Stirling engine that could follow better an ideal Stirling cycle. A Vuilleumier engine, similar to a Stirling engine was reported to find improvement while incorporating dwell in its piston motion [14].

Motion of displacer and piston could hold the key to retrieve lost efficiencies, the forefront when converting theories to practical Stirling engine. Gaining lost efficiencies would produce better and more powerful Stirling engines, making it more attractive to be used as a prime mover, clearly in the effort of seeking cleaner and sustainable power generator. Efforts to closely follow the ideal Stirling cycle's displacer and piston motion showed improvement over conventional sinusoidal motion [19, 24, 25]. These researches had also motivated others to participate into this research area as it focusses on the drive mechanism, complement to existing Stirling engine technology and knowledge.

There are still specific details on motions and dwells that still in need to be investigated. Timing of the motion and dwell events is still unknown and how it would affect the performance of the Stirling engine as it depends on the rate of heat transfer. The inclusive of piston dwell was not present. The objective of this paper is to investigate the use of non-sinusoidal motion of rise-dwell-fall-dwell (RDFD) cycloidal motion to both displacer and piston and to compares that with the conventional sinusoidal motion. The outcome of this investigation contributes to a better understanding of the heat transfer event, retrieving lost efficiencies of Stirling engines and a novel cam drive mechanism.

METHODOLOGY

A Stirling engine test rig was developed for the investigation, as shown in Figure 2. Gamma configuration was selected due to its simplicity in design and requires lesser precision machining compared to beta configuration. Any change to the

motion of displacer will not affect the overall engine volume as an alpha configuration would. A central balanced aluminum flywheel with two face grooved radial cams at either side was designed and fabricated. There were two cam followers to shift the displacer and piston at each side of the Stirling engine. A prony brake dynamometer was used to provide engine loading. Heating was provided to the test rig via DC electric heater, insulated with glass fiber insulation. Cooling is accomplished with an open circuit municipal water, running one way, circulating the water cooling chamber at the cold end. It had a data acquisition system which utilizes a laptop to capture the air pressure in the hot end, cold end and power cylinder as well as positions of both displacer and piston through the use of Picotech 1216 Picolog with PicoScope 6. This setup is similar to the setup of Kato (2016) [34]. Pressure sensors were calibrated against an industrial grade pressure gauge prior conducting the tests. Temperature across 7 points (hot end, cold end, regenerator hot end, regenerator cold end, power cylinder, coolant in and coolant out) of the test rig were monitored and measured with K-type thermocouples coupled to the Picotech thermocouple data logger TC-08. However, the thermocouples we not calibrated as they are only for monitoring purposes and not used to calculate any thermal efficiencies. The schematic diagram can be seen in Figure 3. Table 1 lists the specification of the Stirling engine test rig.

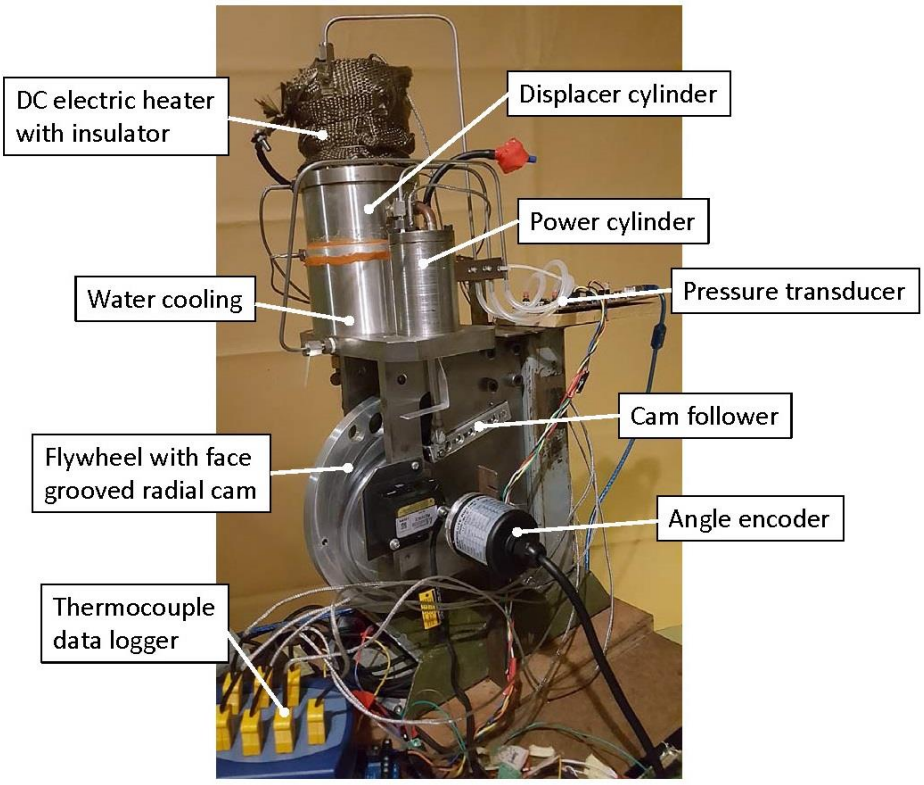

Figure 2. Stirling engine test rig

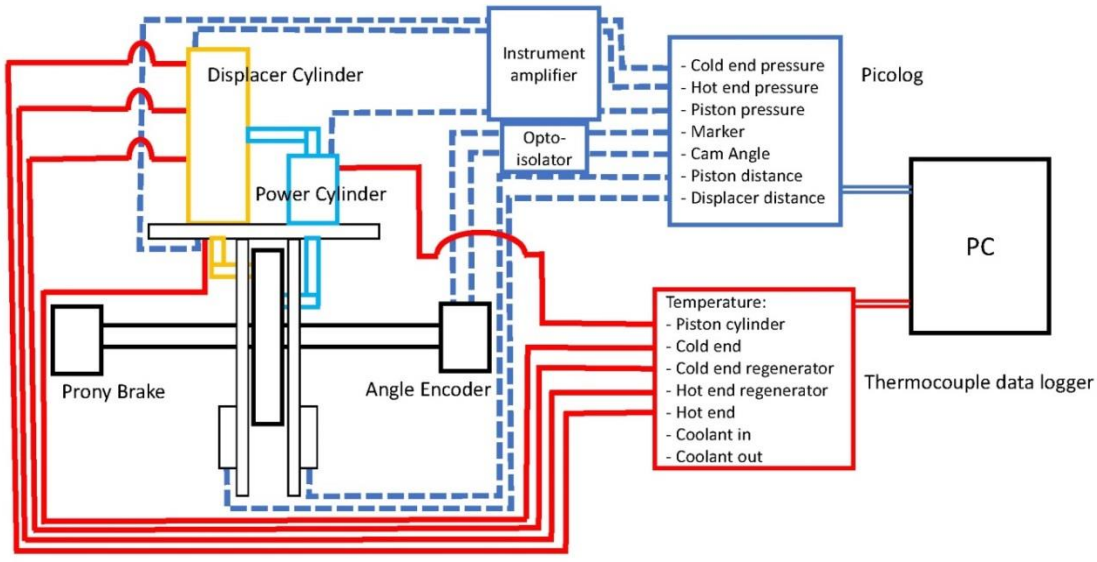

Figure 3. Data acquisition system

Table 1. Specifications of the Stirling engine test rig

Description	Specification
Engine Type / Volume	Gamma / 267 cc
Displacer Cylinder Diameter / Stroke	60 mm / 35 mm
Piston Cylinder Diameter / Stroke	40 mm / 35 mm
Displacer Cylinder	Stainless Steel hot end and Aluminum cold end with Stainless Steel dimpled coil regenerator
Displacer	Thin walled Stainless Steel with Mild steel cap and Stainless Steel shaft
Power Piston Cylinder	Mild Steel
Power Piston	Graphite with Aluminum pivoting system.
Working Fluid	Air

Four cams were fabricated for the investigation. One of the cams was a baseline standard crank shaft sinusoidal movement with 90° phase angle. The other three cams were based on certain design parameter of RDFD. Cycloidal motion was used for all the RDFD as it is a suitable motion choice for high speed application [35] as it compromises for all basic cam requirements including the finite value of jerk. Table 2 describes the specification of cams.

Table 2. Specifications of tested cams

Cam identification	Displacer	Power Piston
Crank	Sinusoidal	Sinusoidal with 90° lagging phase
90_90	90° (Rise) – 90° (Dwell) – 90° (Fall) – 90° (Dwell)	90° (Dwell) – 90° (Rise) – 90° (Dwell) – 90° (Fall)
90_90 Ovrlp	90° (Rise) – 90° (Dwell) – 90° (Fall) – 90° (Dwell)	60° (Dwell) – 120° (Rise) – 60° (Dwell) – 120° (Fall)
135_45 Ovrlp	45° (Rise) – 135° (Dwell) – 45° (Fall) - 135° (Dwell)	15° (Dwell) – 165° (Rise) – 15° (Dwell) – 165° (Fall)

Figure 4 showed the graphical representation of the tested cam profiles where the top represents piston positions and the bottom represents displacer pistons at respective cam angles. The baseline, crank cam replicated movements by a conventional sinusoidal crankshaft with 90° phase angle where both displacer and piston moves in sinusoidal motion with the piston lagged 90° (the thick blue line) after displacer. This cam was the baseline for comparison. The 90_90 cam implemented the RDFD motion and followed the theoretical Stirling cycle displacer and piston motions (thin blue line) where the piston dwells with displacer moves and vice-versa in sequence, as shown in Figure 1. The 90_90 Ovrlp cam had the same displacer motion of the 90_90 cam but included a 15° overlap in the piston motion at the end of the two (2) displacer dwell periods (thin dashed green line), prolonging the piston's expanding and compressing motion. This was a development from the 90_90 cam. The 135_45 Ovrlp cam further expanded the displacer dwell from 90° to 135° while having the same 15° overlap (thin red line), thus prolonging the up and down motion period of piston. All these three non-sinusoidal cams were expected to affect the performance of the Stirling engine similarly to Briggs (2015) [28] and Gopal (2012) [29]. The difference between this work and previous work is the addition of piston dwell which could provide constant volume regeneration. Implementation of dwell in the displacer's motion prolongs the time for heat transfer as well as containing and maintaining the most amount of working fluid's mass at each heat exchangers, increased the amount of heat transfer in and out of the working fluid, the similar manner an ideal Stirling engine would perform, affecting the performance of the Stirling engine.

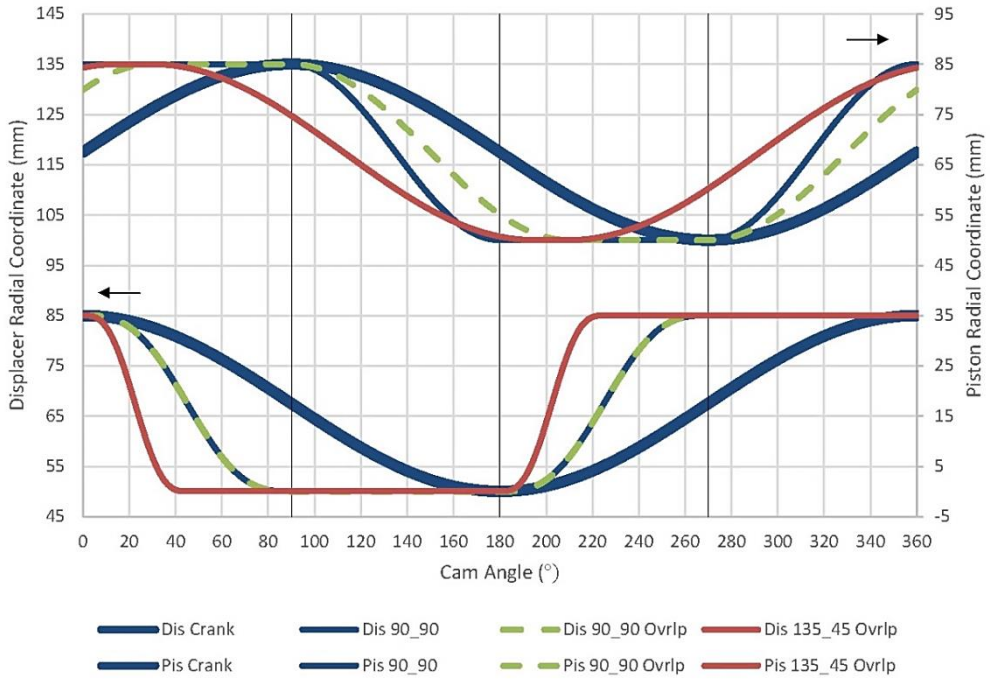

Figure 4. Cam profiles of all tested cams

Test Procedure

Test procedure for testing each cams was as follow. Heating power was set at 350 W. A warmed up period of the engine with the coolant flowing within was used. Upon reaching desired temperature (cold end temperature at 40 ±0.5 °C) and the targeted engine speed (through adjustment of prony brake dynamometer), data of 3 pressures (hot end, cold end and power cylinder), positions of displacer and piston as well as 2 encoder pulses (1 pulse / revolution and 180 pulses /revolution), were recorded for 10 consecutive cycles. Data was then post-processed using a spreadsheet where it is filtered and processed to obtain pressure and volume. Since only the cams were changed for every test (all other components remain the same), comparisons were direct. For data analysis, indicated pressure versus cam angle and PV diagram were plotted. Values of indicated mean effective pressure, power and thermal efficiency were calculated from work, which is based on the internal area of PV diagram [2].

RESULTS AND DISCUSSION

Figure 5, 6 and 7 showed the change of pressure in the Stirling engine test rig and the cold end volume (under line C), hot end volume (between line CH and C) and piston volume (between line CHP and CH) versus cam angles of all tested cams. As illustrated in Figure 5, the baseline crank cam presents a pressure profile similar to a sinusoidal profile as air was shuttled back and forth the hot and cold end. The 90_90 cam exhibits a larger pressure range (difference in indicated pressure) compared to the baseline crank cam, 27,993 Pa versus 14,512 Pa. As all conditions of heating power input, cold end temperature and the physical engine were identical in both cases, this change can only be coming from the use of dwells in the 90_90 cam that had improved its heat transfer to the working fluid. This outcome was found similar to the earlier research [19, 24, 25]. As both the displacer and piston had its own dwell, it is difficult to separate each contribution to this improvement. Displacer dwell had prolonged the trapping and exposing large amount of air mass to either end of the displacer cylinder for heat exchange. Piston dwell allowed the displacer to shuttles air without the change in engine volume. Both of these phenomenon could have contributed to the rise in pressure range.

Usage of this cam also gave two sets of unnecessary pressure fluctuations when the displacer nears the end of its dwell period and the piston nearing TDC or BDC. During this time, the piston travels slower at the beginning and the ending of its motion, which is a characteristic of cycloidal motion to minimized acceleration in RDFD motion. This lowered acceleration moves very little of the piston, stagnating the air trapped in the displacer cylinder (end of displacer dwell). As heat is constantly transferred with little or no change in engine volume, pressure can only continue to rise if rising or drop if dropping until the engine volume changes due to the movement of piston, countering the trend of pressure change. This is observed as a fluctuation of pressure and it is not desired. Fluctuations in pressure showed signs of being inefficient. In order to perform best, pressure rise and fall should be smooth, similar to the baseline. Rather than the heat is absorbed and dispersed smoothly, it is absorbed and dispersed excessively, wasting the heat away.

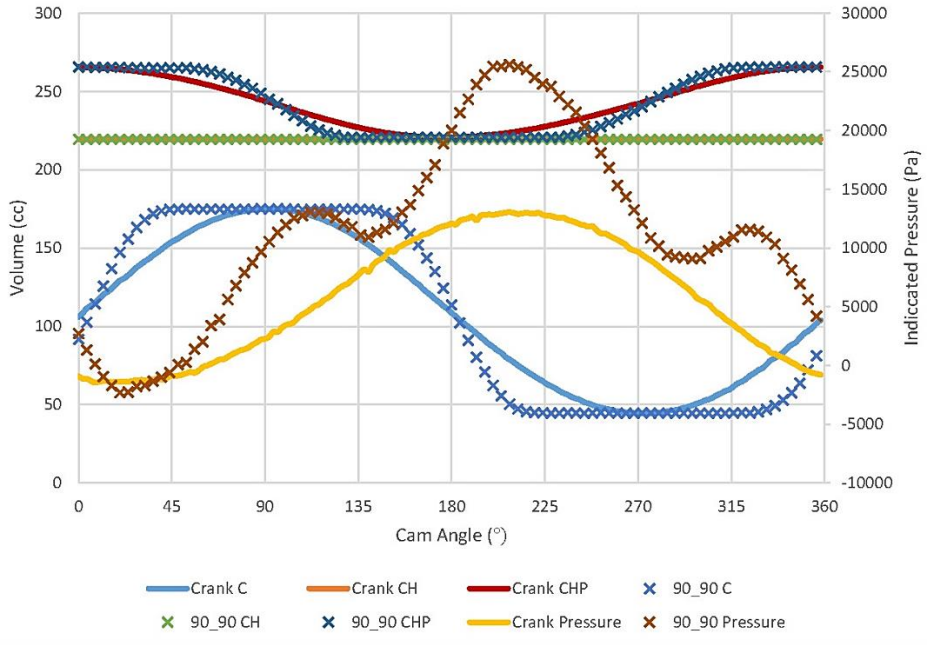

Figure 5. Pressure profile and engine volume versus cam angle comparison between 90_90 cam and baseline crank cam

The outcome from the 90_90 cam was found that dwell improves the Stirling engine performance but the timing of events was unfavorable as there pressure fluctuations. This has led to the development of the 90_90 Ovrlp cam. This cam had incorporated 15° of piston motion overlap at the ending of both the displacer dwell since the fluctuations only occurred at the end of each dwell while the front end was left identical with the 90_90 cam. The cam was tested and the test results can be seen in Figure 6. This cam design reduced the effect of pressure fluctuation found in the testing of 90_90 cam. This was achieved by minimizing the period of air stagnation with the overlap of motion. Pressure change was found smoother when compared to the 90_90 cam while still exhibits larger pressure range than the baseline crank cam (26,220 Pa versus 14,512 Pa) but lesser than the 90_90 cam (27,993 Pa). All in all, usage of 90_90 Ovrlp cam successfully smoothened the pressure profile, thus making the engine performed better which can be seen in the discussion of IMEP later.

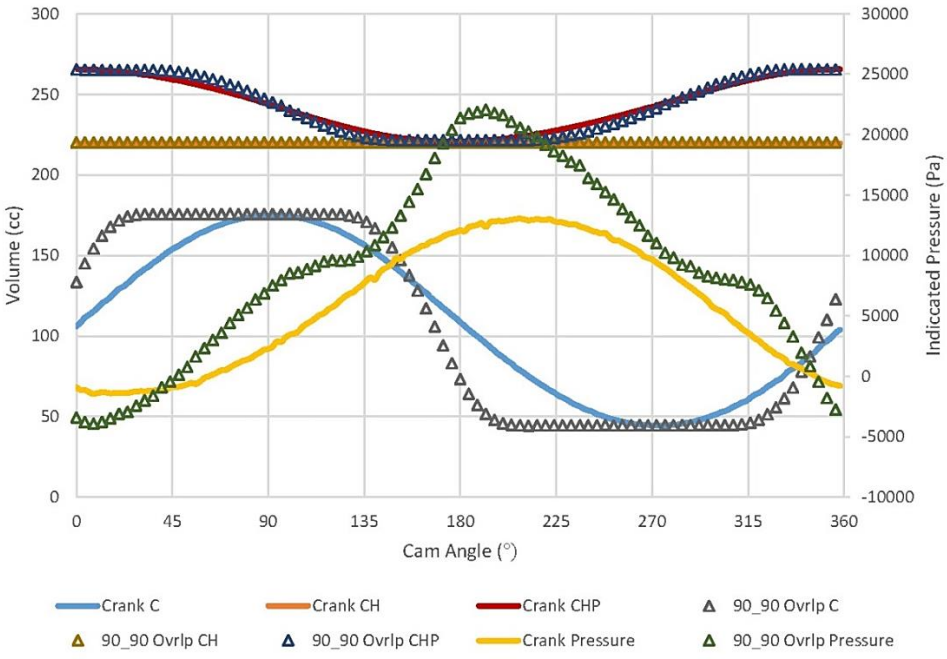

Figure 6. Pressure profile and engine volume versus cam angle comparison between 90_90 Ovrlp cam and baseline crank cam

The last tested cam was the 135_45 Ovrlp cam. As shown in Figure 7, the pressure range by the 135_45 Ovrlp cam was the largest among all RDFD cams, valued at 27905 Pa. This best performance was achieved due to the usage of extended displacer dwell of 135° while retaining the same overlap of 15°. This extended dwell had allowed larger amount of heat transfer compared to 90° dwell, causing the pressure to rise up to the mentioned value. There were no pressure fluctuations occurred, as indicated in Figure 7 and this proved the overlap of 15° able to suppress it. Overlap of motion manage to keep air in motion rather than being stagnant, reducing and eliminating pressure fluctuation. All in all, the 135_45 Ovrlp cam managed to enlarged its pressure range from 14,512 Pa of the baseline sinusoidal motion as much as 92.29% by only implementing non-sinusoidal RDFD motion, without any change to the Stirling engine. True to the earlier finding [8 – 10, 25] that incorporation of dwell had improved the Stirling engine with conventional sinusoidal motion. The use long displacer dwell of 135° was found desired and the timing was to include piston motion overlap prior to the end of displacer dwell to ensure smooth transition of pressure for maximum benefit.

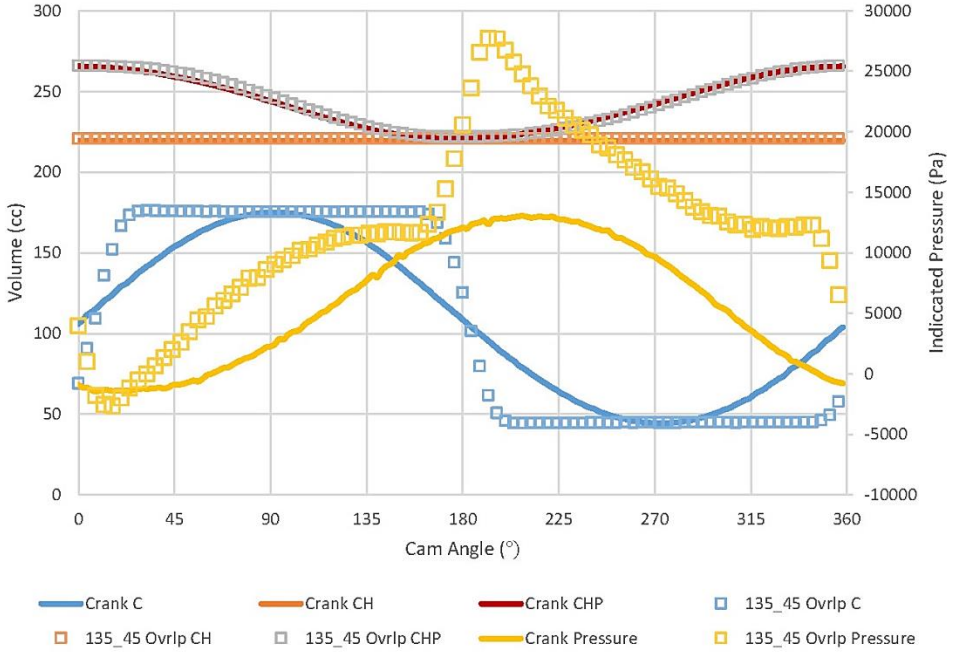

Figure 7. Pressure profile and engine volume versus cam angle comparison between 135_45 Ovrlp cam and baseline crank cam

Figure 8 showed the PV diagram for each of the tested cams. The crank cam gave the classical PV diagram of a real Stirling engine. The non-sinusoidal RDFD cams of 90_90 cam, 90_90 Ovrlp cam and 135_45 Ovrlp cam all showed the ability to gain constant volume regeneration during the piston dwells at top dead center (TDC) and bottom dead center (BDC). Implementation of piston dwell was successfully implemented and able to obtain constant volume regeneration. During this moment, the displacer shuttled air from the ends (hot to cold or cold to hot) passing through the regenerator, permitting constant volume heat regeneration while the piston dwelled. Pressure in the engine changed as heat was exchanged at the regenerator and as a result, it gained a large pressure range. This obtainment of constant volume regeneration is unheard of.

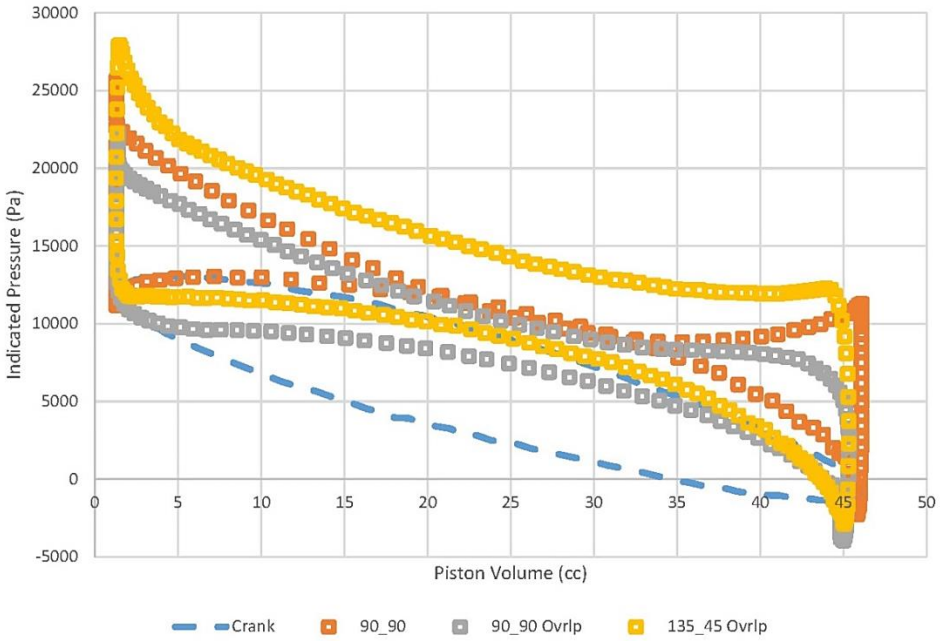

Figure 8. PV diagram for tested cams

The 90_90 cam had two (2) sharp pressure fluctuations (ie. overshot), at the ending of its constant volume regeneration processes, as shown in Figure 8, represented by the orange square. These were the same two pressure fluctuations occurred during the motion transitions, as shown in Figure 5. These high pressure fluctuations did not produce any work (zero volume change) and therefore contributed to the smaller indicated mean effective pressure (IMEP) of 2,896.50 Pa for the 90_90 cam compared to the baseline crank cam IMEP of 5,300.82 Pa. The 90_90 Ovrlp cam had reduced the pressure fluctuations with its 15° overlap and as a result, larger IMEP of 4,721.80 Pa, affirming the importance of using overlapping. However, it was still under performing when compared to the baseline crank cam. The 135_45 Ovrlp cam performed the best with IMEP of 7,534.59 Pa. This outcome showed the importance of implementing large sized displacer dwell and timing to include overlap in the non-sinusoidal RDFD motion.

The compression and expansion processes of the RDFD cams all exhibit similar shape but charted a different path, as illustrated in Figure 8. This condition was unique as the usage of cam angle overlap as well as the period for air exposed to the hot and cold end (dwell) were different from the crank cam. To illustrate this point, the gradient of the whole PV diagram of each tested cams were charted, as shown in Figure 9. Small values of either positive or negative gradient indicated the segment of PV diagram was almost horizontal or parallel to the volume axis, which was vital for creating larger IMEP. Figure 9 showed that the crank cam gave mostly small gradient values for its PV diagram of almost oval shaped. All of the RDFD cams exhibits large change of gradients in the angles especially nearing 0° / 360° and 180°, which was cam angle ranges for which the piston dwelled and the displacer shuttled air (constant volume regeneration period), as shown in Figure 5, 6 and 7. The rest of the segments were the compression and expansion period, which lies around 90° and 270°.

From Figure 9, within the region around 90° and 270°, the 90_90 cam had the largest change in gradient within this compression and expansion period, which was not ideal for generating work. Gradient change for the 90_90 Ovrlp cam was smaller than the 90_90 cam, an improvement over the latter cam. The 135_45 Ovrlp cam gradient range almost matched the 90_90 Ovrlp but the gradient range spread over wider cam angles, followed the displacer dwell segment. This affirmed the implementation of overlapping reduces pressure fluctuations and increased IMEP. Usage of longer displacer dwell was beneficial to produce larger IMEP by prolonging the exposure of working gas to either the hot or cold end of the displacer cylinder which ultimately increased heat transfer.

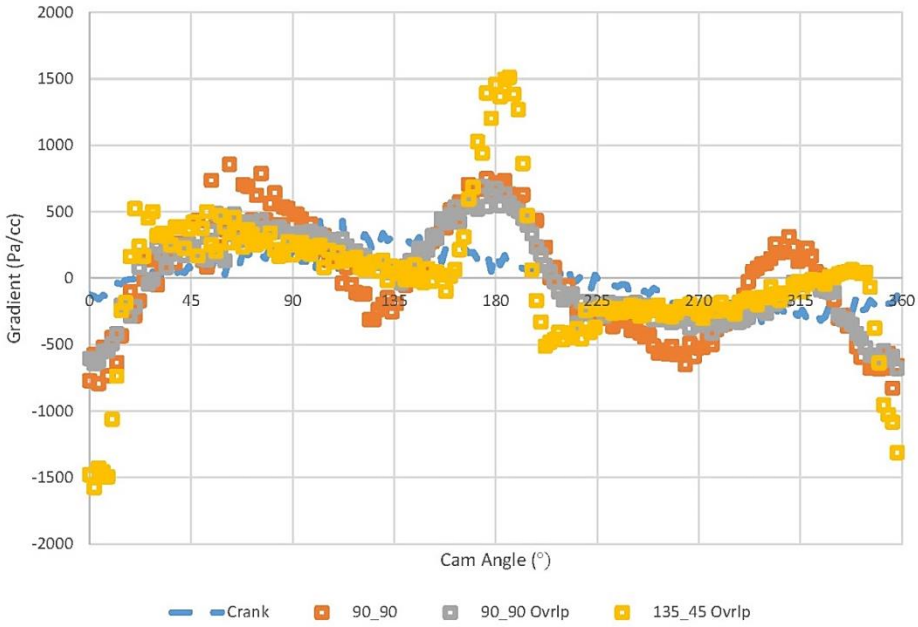

Figure 9. Gradient of PV diagram

Table 3 summarized the overall performance of the Stirling engine. It was found that usage of dwell to be beneficial in generating more power and more efficient as showed in previous researches[19, 24, 25]. However, having similar to its theorized motion (as in the 90_90 cam) did not bring any improvements, as found through earlier researches [3, 23]. The addition of cam overlap improved performance compared with no overlap with the same amount of displacer dwell, as seen in the comparison between 90_90 Ovrlp cam and 90_90 cam. Among these four cams, the best performing cam was the 135_45 Ovrlp cam. It was found that thermal efficiency increased by 36.07% compared to the baseline sinusoidal crank cam.

Table 3. Performance comparison

Cam	IMEP (Pa)	Power (W)	Thermal Efficiency (x 10^{-4})
Crank	5,300.82	0.448	12.81
90_90	2,896.50	0.224	6.38
90_90 Ovrlp	4,721.80	0.380	10.79
135_45 Ovrlp	7,534.59	0.613	17.43

CONCLUSIONS

An experimental investigation to compare sinusoidal motion to the non-sinusoidal RDFD motion in a Stirling engine was performed. The outcome showed that the application of displacer dwell had enhanced heat transfer by prolonging the time for the working fluid to be trapped in the ends of the heat exchanger while dwell at piston contributed to the creation of constant volume regeneration by permitting the displacer to shuttle the working fluid through the regenerator when the piston dwells. Slight overlapping motion of displacer and piston was vital to smoothen the motion of working fluid within the engine at the end of the displacer dwell, reducing air stagnation that cause pressure fluctuation in the cycle. Usage of non-sinusoidal RDFD motion for both displacer and piston was best with the 135_45 Ovrlp cam as it enhanced more than 36% in thermal efficiency compared to baseline conventional sinusoidal crank cam. This experimental investigation had demonstrated the relationship between displacer dwell period and the timing for displacer and piston motion overlapping to the ability to transfer heat and consequently engine performance. This new found approach could contribute to the building of improved Stirling engines through the use of a novel cam drive mechanism, complementing and enhancing existing Stirling engine design and technology. However, further work is needed to fine-tune the displacer and piston motion in terms of its overlapping, timing and duration to develop larger, more powerful and more significant prototypes.

ACKNOWLEDGMENTS

The author would like to thank Universiti Tunku Abdul Rahman for the support given to enable this research to be conducted through the UTAR Research Fund (Project no.: IPSR/RMC/UTARRF/2015-C2/W03).

REFERENCES

[1] D. G. Thombare and S. K. Verma, "Technological development in the Stirling cycle engines," *Renewable and Sustainable Energy Reviews*, vol. 12, no. 1. pp. 1–38, Jan. 2008, doi: 10.1016/j.rser.2006.07.001.

[2] Y. A. Cengel and M. A. Boles, *Thermodynamics: An Engineering Approach*, 5th ed. Boston: McGraw-Hill, 2004.

[3] L. Červenka, "Idealization of The Real Stirling Cycle," *J. Middle Eur. Constr. Des. Cars*, vol. 14, no. 3, 2017, doi: 10.1515/mecdc-2016-0011.

[4] C. C. Kwasi-Effah, A. I. Obanor, and F. A. Aisien, "Stirling Engine Technology : A Technical Approach to Balance the Use of Renewable and Non-Renewable Energy Sources," *Am. J. Renew. Sustain. Energy*, vol. 1, no. 3, 2015.

[5] M. H. Ahmadi, M. A. Ahmadi, and F. Pourfayaz, "Thermal models for analysis of performance of Stirling engine: A review," *Renewable and Sustainable Energy Reviews*, vol. 68. 2017, doi: 10.1016/j.rser.2016.09.033.

[6] G. Xiao *et al.*, "Design optimization with computational fluid dynamic analysis of β-type Stirling engine," *Appl. Therm. Eng.*, vol. 113, 2017, doi: 10.1016/j.applthermaleng.2016.10.063.

[7] Y. Timoumi, I. Tlili, and S. Ben Nasrallah, "Performance optimization of Stirling engines," *Renew. Energy*, vol. 33, no. 9, 2008, doi: 10.1016/j.renene.2007.12.012.

[8] Y. Timoumi, I. Tlili, and S. Ben Nasrallah, "Design and performance optimization of GPU-3 Stirling engines," *Energy*, vol. 33, no. 7. 2008, doi: 10.1016/j.energy.2008.02.005.

[9] R. Gheith, H. Hachem, F. Aloui, and S. Ben Nasrallah, "Experimental and theoretical investigation of Stirling engine heater: Parametrical optimization," *Energy Convers. Manag.*, vol. 105, 2015, doi: 10.1016/j.enconman.2015.07.063.

[10] M. Ni *et al.*, "Improved Simple Analytical Model and experimental study of a 100 W β-type Stirling engine," *Appl. Energy*, vol. 169, 2016, doi: 10.1016/j.apenergy.2016.02.069.

[11] D. J. Shendage, S. B. Kedare, and S. L. Bapat, "Cyclic analysis and optimization of design parameters for Beta-configuration Stirling engine using rhombic drive," *Appl. Therm. Eng.*, vol. 124, 2017, doi: 10.1016/j.applthermaleng.2017.06.075.

[12] M. F. Zainudin, R. A. Bakar, G. L. Ming, T. Ali, and B. A. Sup, "Thermodynamic cycle evaluation of rhombic drive beta-configuration Stirling engine," in *Energy Procedia*, 2015, vol. 68, doi: 10.1016/j.egypro.2015.03.273.

[13] Z. M. Farid, A. B. Rosli, and K. Kumaran, "Effects of phase angle setting, displacement, and eccentricity ratio based on determination of rhombic-drive primary geometrical parameters in beta-configuration Stirling engine," in *IOP Conference Series: Materials Science and Engineering*, 2019, vol. 469, no. 1, doi: 10.1088/1757-899X/469/1/012047.

[14] H. Chen, C. C. Lin, and J. P. Longtin, "Performance analysis of a free-piston Vuilleumier heat pump with dwell-based motion," *Appl. Therm. Eng.*, vol. 140, 2018, doi: 10.1016/j.applthermaleng.2018.05.028.

[15] B. Cullen and J. McGovern, "Development of a theoretical decoupled Stirling cycle engine," *Simul. Model. Pract. Theory*, vol. 19, no. 4, 2011, doi: 10.1016/j.simpat.2010.06.011.

[16] Y. Kato, "Indicated diagrams of low temperature differential Stirling engines with channel-shaped heat exchangers," *Renew. Energy*, vol. 103, 2017, doi: 10.1016/j.renene.2016.11.026.

[17] A. R. Tavakolpour-Saleh, S. H. Zare, and H. Bahreman, "A novel active free piston Stirling engine: Modeling, development, and experiment," *Appl. Energy*, vol. 199, 2017, doi: 10.1016/j.apenergy.2017.05.059.

[18] M. Tarawneh, F. Al-Ghantian, M. A. Nawafleh, and N. Al-Kloub, "Numerical Simulation and Performance Evaluation of Stirling Engine Cycle," *Jordan J. Mech. Ind. Eng.*, vol. 4, pp. 615–628, 2010.

[19] M. Craun and B. Bamieh, "Optimal periodic control of an ideal stirling engine model," *J. Dyn. Syst. Meas. Control. Trans. ASME*, vol. 137, no. 7, 2015, doi: 10.1115/1.4029682.

[20] M. T. García, E. C. Trujillo, J. A. V. Godiño, and D. S. Martínez, "Thermodynamic model for performance analysis of a Stirling engine prototype," *Energies*, vol. 11, no. 10, 2018, doi: 10.3390/en11102655.

[21] R. Li, L. Grosu, and D. Queiros-Condé, "Losses effect on the performance of a Gamma type Stirling engine," *Energy Convers. Manag.*, vol. 114, 2016, doi: 10.1016/j.enconman.2016.02.007.

[22] D. Erol, H. Yaman, and B. Doğan, "A review development of rhombic drive mechanism used in the Stirling engines," *Renewable and Sustainable Energy Reviews*, vol. 78. 2017, doi: 10.1016/j.rser.2017.05.025.

[23] S. Ranieri, G. A. O. Prado, and B. D. MacDonald, "Efficiency reduction in stirling engines resulting from sinusoidal motion," *Energies*, vol. 11, no. 11, 2018, doi: 10.3390/en11112887.

[24] A. Ibrahim, P. L. Chong, V. Rajasekharan, M. M. Ali, O. S. Zaroong, and N. O. Ahmed, "Investigation of the effect of different materials on convective heat transfer," *J. Mech. Eng. Sci.*, vol. 14, no. 2, 2020, doi: 10.15282/jmes.14.2.2020.08.0520.

[25] A. A. Mohamed and O. Younis, "Performance of drop shaped pin fin heat exchanger with four different fin dimensions," *J. Mech. Eng. Sci.*, vol. 14, no. 2, 2020, doi: 10.15282/jmes.14.2.2020.31.0543.

[26] M. I. N. Ma'Arof, G. T. Chala, H. Husain, and M. S. S. Mohamed, "Influence of fins designs, geometries and conditions on the performance of a plate-fin heat exchanger-experimental perspective," *J. Mech. Eng. Sci.*, vol. 13, no. 1, 2019, doi: 10.15282/jmes.13.1.2019.02.0372_rfseq1.

[27] D. Sahel, H. Ameur, and M. Mellal, "Effect of tube shape on the performance of a fin and tube heat exchanger," *J. Mech. Eng. Sci.*, vol. 14, no. 2, 2020, doi: 10.15282/jmes.14.2.2020.13.0525.

[28] M. Briggs, "Improving Free-Piston Stirling Engine Power Density," Case Western Reserve University, 2015.

[29] V. K. Gopal, "Active Stirling Engine," University of Canterbury, 2012.

[30] H. W. Fang, K. E. Herold, H. M. Holland, and E. H. Beach, "Novel Stirling engine with an elliptic drive," in *Proceedings of the Intersociety Energy Conversion Engineering Conference*, 1996, vol. 2, doi: 10.1109/iecec.1996.553887.

[31] J. Podešva and Z. Poruba, "The Stirling engine mechanism optimization," *Perspect. Sci.*, vol. 7, 2016, doi: 10.1016/j.pisc.2015.11.052.

[32] M. Jaśkiewicz, W. Sadkowski, M. Marciniewski, K. Olejnik, and J. Stokłosa, "Proposal of the New Concept of the Stirling Engine," *Sci. Journals Marit. Univ. Szczerin*, vol. 35, no. 107, pp. 32–37, 2013.

[33] J. D. Van de Ven, "Mobile hydraulic power supply: Liquid piston Stirling engine pump," *Renewable Energy*, vol. 34, no. 11. 2009, doi: 10.1016/j.renene.2009.01.020.

[34] Y. Kato, "Indicated diagrams of a low temperature differential Stirling engine using flat plates as heat exchangers," *Renew. Energy*, vol. 85, 2016, doi: 10.1016/j.renene.2015.07.053.

[35] R. L. Norton, *Design of Machinery: an Introduction to the Synthesis and Analysis of Mechanisms and Machines*, 5th ed. New York: McGraw-Hill, 2012.